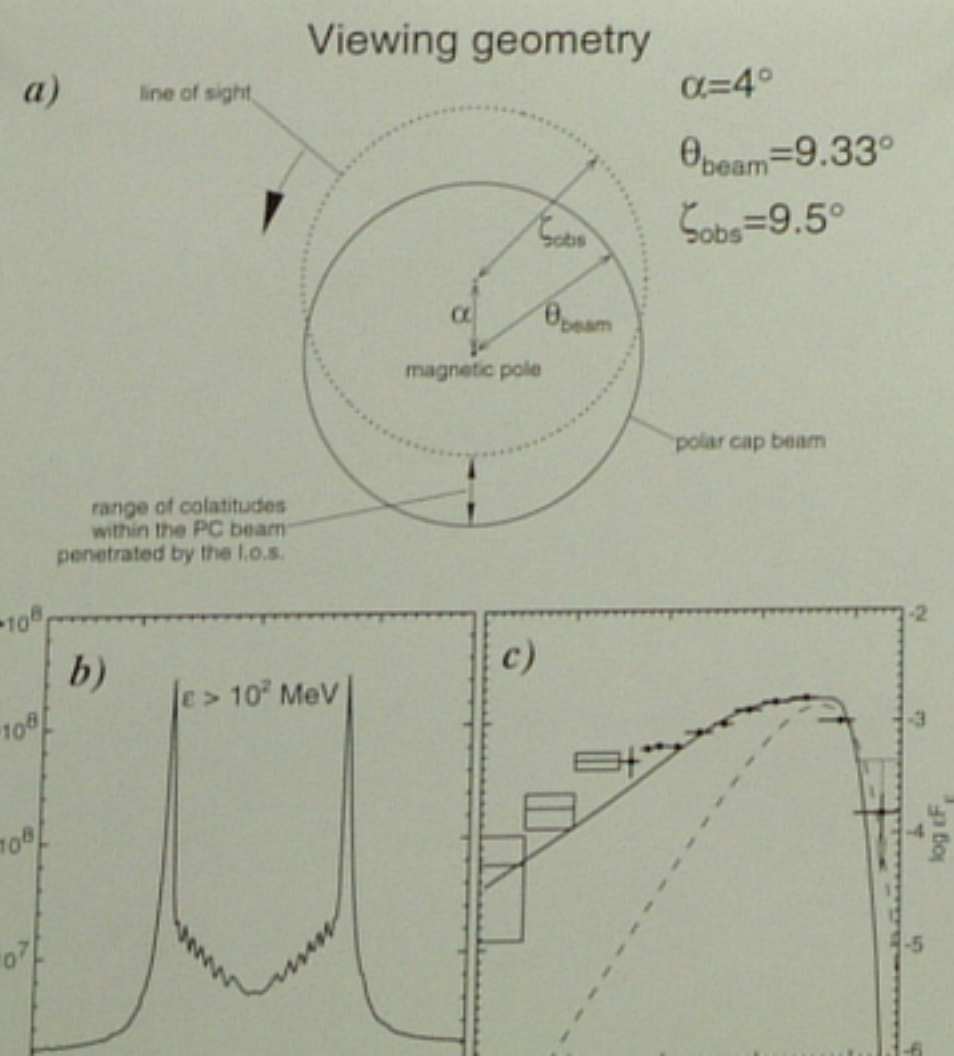


SIGNATURES OF PULSAR POLAR-GAP EMISSION AT THE HIGH-ENERGY SPECTRAL CUTOFF

J. Dyks and B. Rudak

Nicolaus Copernicus Astronomical Center, Toruń, POLAND



2 Weakening of the leading peak

According to the polar cap model, the characteristic double-peak gamma-ray pulse profiles of pulsars arise as follows: when the line of sight enters the polar cap beam the leading peak is produced (LP); crossing inner parts of the hollow beam gives the bridge emission between the two peaks, and leaving the beam gives the trailing peak (TP) (see Fig. 2a and 3a).

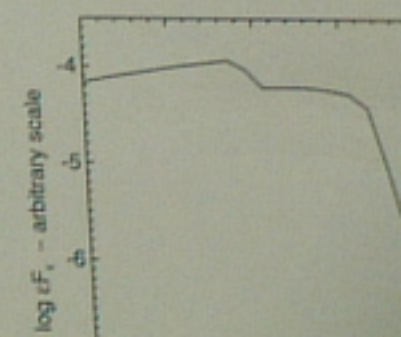
Rotation of magnetosphere enhances the magnetic absorption of photons in the leading peak and weakens the absorption of the trailing peak (Dyks, Rudak 2002). This may be easily understood by inspection of Fig. 4, which shows the trajectory of leading peak photons (dashed curve on the left) and trailing peak photons (dashed curve on the right) in the frame rigidly corotating with the star.

Therefore, the leading peak in a pulse profile disappears at a lower photon energy than the trailing peak, an effect noticed among the brightest EGRET pulsars (Thompson 2001). Fig. 5 shows this effect for the nearly aligned model of the Vela pulsar (see two lowermost panels in the middle column).

Due to the stronger absorption at the leading peak, a higher number of low-energy synchrotron photons emerges at the LP than at the TP. This is the reason for a dominance of the LP over the TP below $\sim 100 \text{ MeV}$, noticeable in Fig. 5. A qualitatively similar inversion of

3 Step-like spectrum

For the nearly-aligned model of Vela, shown in Fig. 5, the leading peak can be discerned only when acceleration takes place at high altitudes, where the local corotation speed is assumed $h = 4R_{NS}$ in Fig. 5). However, for millisecond pulsars with high inclination angles α of magnetic dipole, the high-energy cutoff's energy for the leading and for the trailing peak is pronounced, and may be noticeable even in the phase-averaged spectrum as a step nearby the HE cutoff. In the spectrum of Vela, a step occurs at around 10^5 MeV , and the "ultimate" cutoff is at 10^6 MeV . Below the step the spectrum consists of the leading and the trailing peak, whereas above the step only the trailing peak contribute. At the step the flux drops by a factor of ~ 2 .



We investigate 4 unique features of pulsar gamma-ray emission nearby the high-energy cutoff above 10 GeV, as predicted by the polar cap model.

1 Super-exponential shape of the high-energy cutoff

There exists a widespread opinion that the polar cap model predicts very sharp cutoff (super-exponential) at the high-energy (HE) end of pulsar spectrum (Harding 2001; de Jager 2002). We anticipate that GLAST will be able to discern this signature in phase-averaged pulsar spectra. However, the situation is in fact not so simple. The shape of high-energy cutoff in pulsar spectra clearly depends on viewing geometry: in the off-beam case (when the line of sight misses the highest energy gamma-ray beam) the cutoff has a simple exponential shape due to the upper limit in the spectrum of particles which emit observable photons. Moreover, even in the case of the on-beam geometry (when the line of sight samples the polar cap) *the cutoff in the phase-averaged spectrum DOES NOT have to assume a sharp, super-exponential shape.*

A simple reason for this can be deduced from Figs. 1-3: for radiation emitted at different distances from magnetic axis (magnetic colatitudes) the sharp cutoff occurs at different photon energies (often called "escape energies", see Fig. 1). In the course of pulsar rotation the line of sight samples a range of magnetic colatitudes, and therefore, the phase-averaged spectrum is composed of many spectra with different positions of the cutoff. When the range of sampled colatitudes is narrow (Fig. 2a) the phase averaged spectrum (solid line in Fig. 2c) does have much sharper cutoff than the simple exponential one (dashed line in Fig. 2c). For a broader range of sampled colatitudes, however, (Fig. 3), the cutoff in the phase-averaged spectrum may look exactly like a simple exponential (Fig. 3c).

Conclusion: the shape of the high-energy cutoff in the phase-averaged spectra depends on the viewing geometry and does not have to be super-exponential even in the on-beam case. To observe the sharp cutoff it is necessary to investigate phase-resolved spectra or to have the good luck of appropriate viewing geometry.

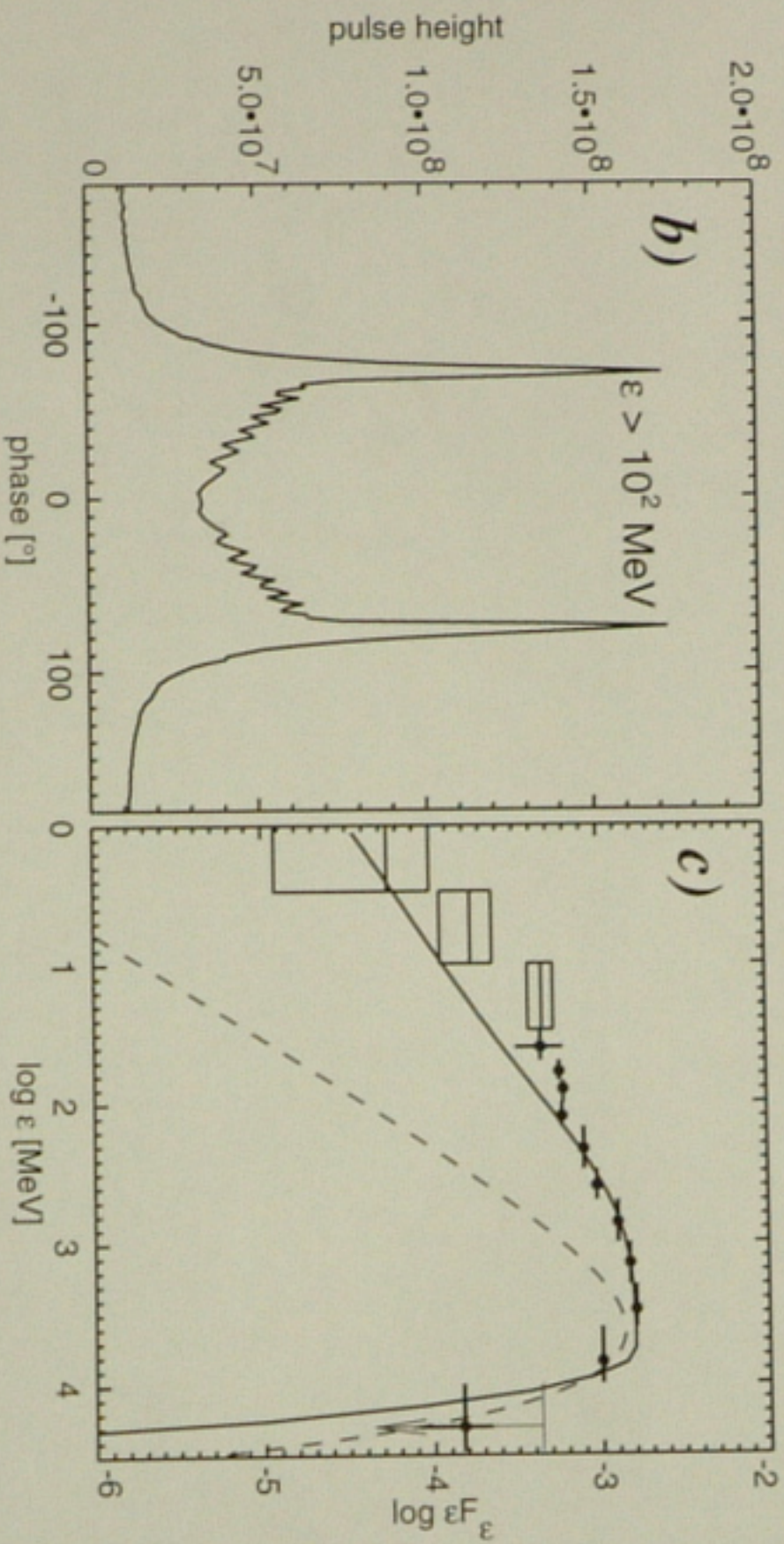
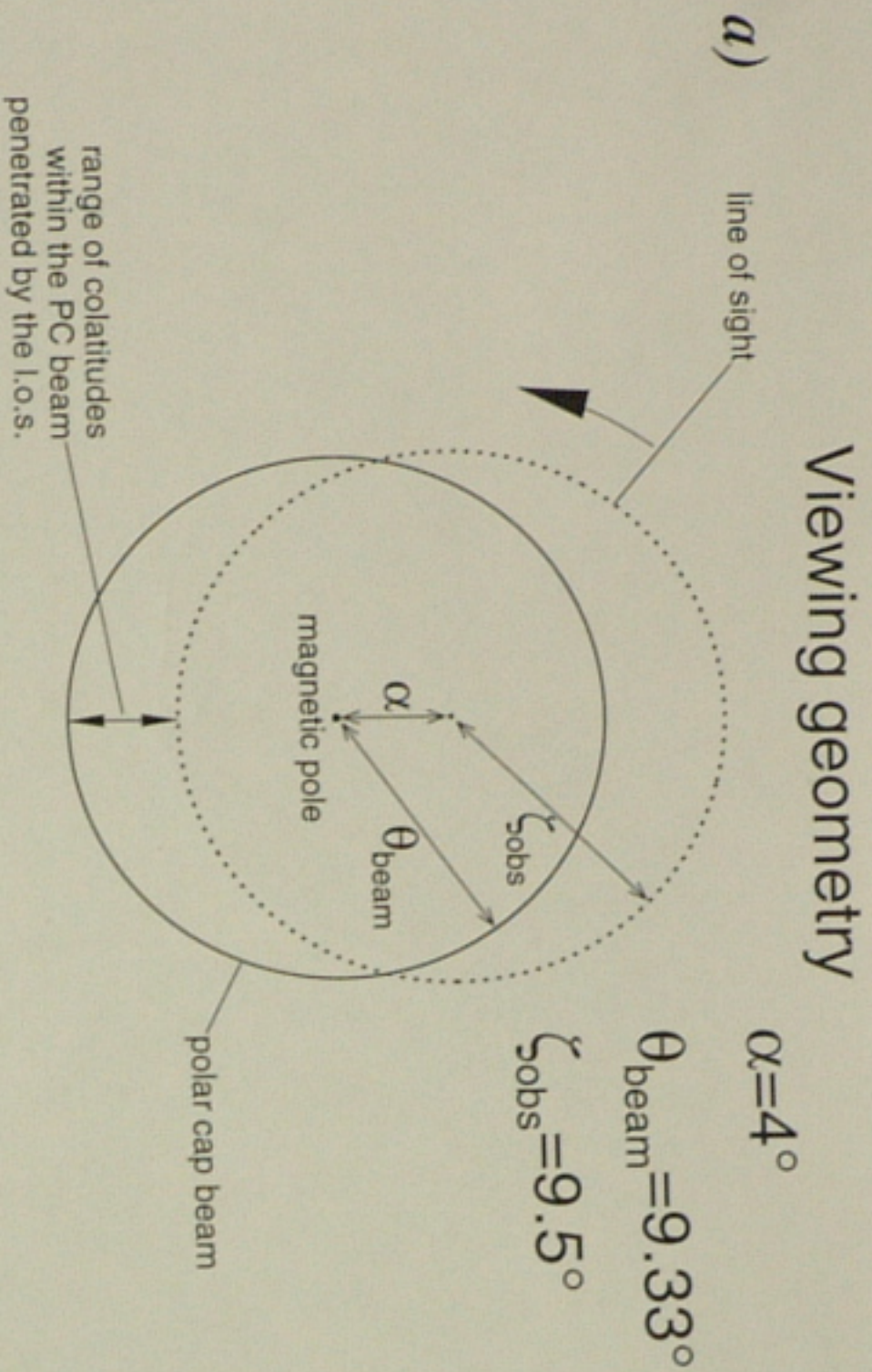


Figure 2: **a)** Viewing geometry assumed to calculate the profile and the spectrum shown in panels **b** and **c**. The line of sight crosses the polar cap beam (solid circle) along the dotted trajectory. **b)** Pulse profile calculated for $\epsilon > 10^2$ MeV. **c)** Phase-averaged spectrum (solid line) overplotted on COMPTEL and EGRET data for the Vela pulsar. An instantaneous spectrum of CR with exponential cutoff due to monoenergetic particles is shown for reference (dashed line). The modelled spectrum has a much sharper cutoff than the simple exponential.

Viewing geometry

a)

line of sight

$\alpha = 7.6^\circ$

different positions of the cutoff. When the range of sampled colatitudes is narrow (Fig. 2a) the phase averaged spectrum (solid line in Fig. 2c) is narrow (Fig. 2a) the phase averaged spectrum (solid line in Fig. 2c) does have much sharper cutoff than the simple exponential one (dashed line in Fig. 2c). For a broader range of sampled colatitudes, however, (Fig. 3), the cutoff in the phase-averaged spectrum may look exactly like a simple exponential (Fig. 3c).

Conclusion: the shape of the high-energy cutoff in the phase-averaged spectra depends on the viewing geometry and does not have to be super-exponential even in the on-beam case. To observe the sharp cutoff it is necessary to investigate phase-resolved spectra or to have the good luck of appropriate viewing geometry.

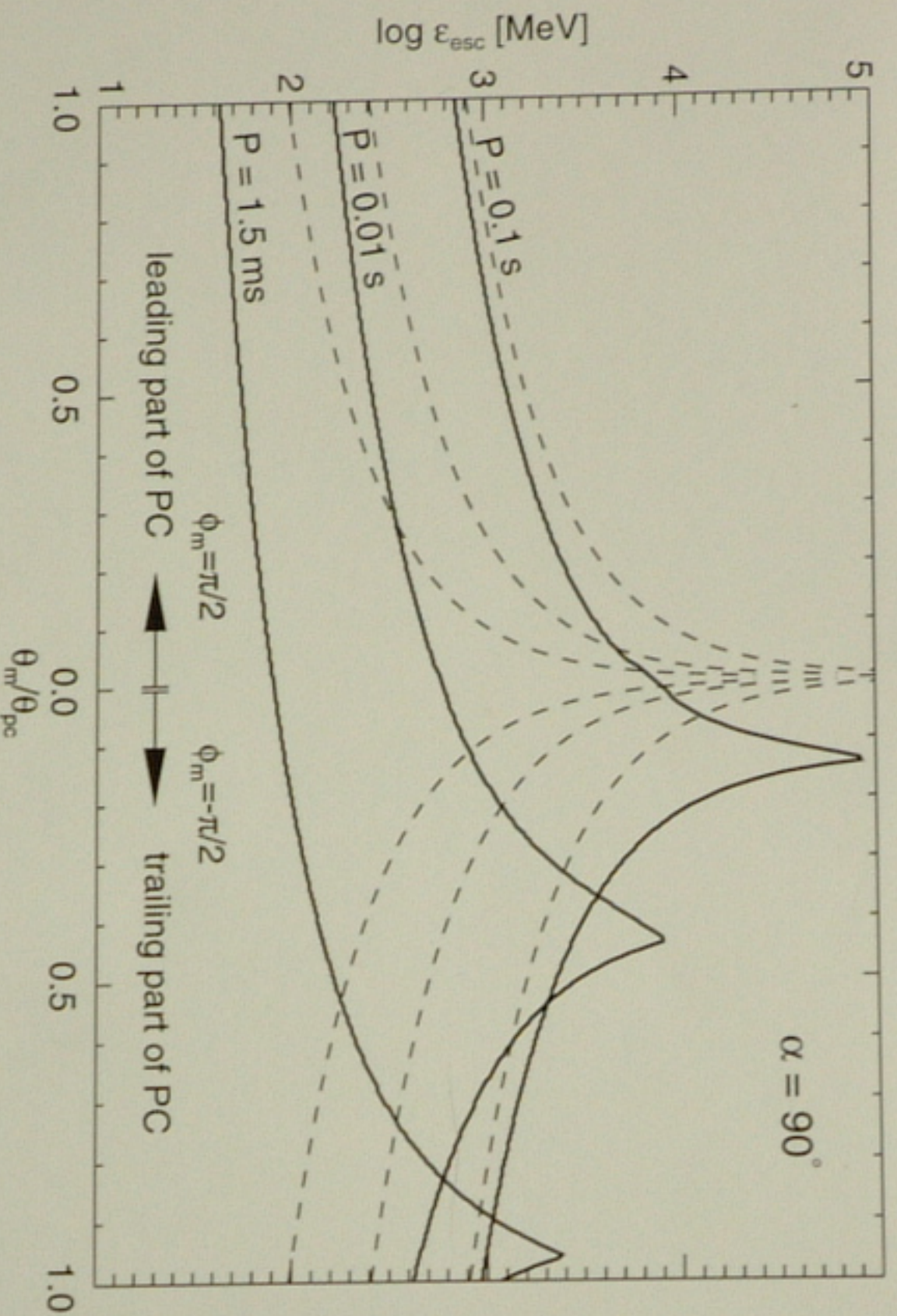


Figure 1: The escape energy ϵ_{esc} of photons from the polar cap surface of an orthogonal rotator with $B_{\text{pc}} = 10^{12} \text{ G}$ is shown as a function of normalized magnetic colatitude $\theta/\theta_{\text{pc}}$ of the emission points. The points are assumed to lay along the cross-section of the polar cap surface with the equatorial plane of rotation, thus location of each point is determined by $\theta/\theta_{\text{pc}}$ in the range $[0, 1]$, and the magnetic azimuth ϕ_m equal either to $\pi/2$ (for the leading half of the polar cap) or $-\pi/2$ (for the trailing half). Three solid lines are labelled with the corresponding spin periods P of 0.1 s, 10 ms, and 1.5 ms. Each solid line is accompanied by a dashed line calculated for the case when rotational effects are ignored.

Viewing geometry

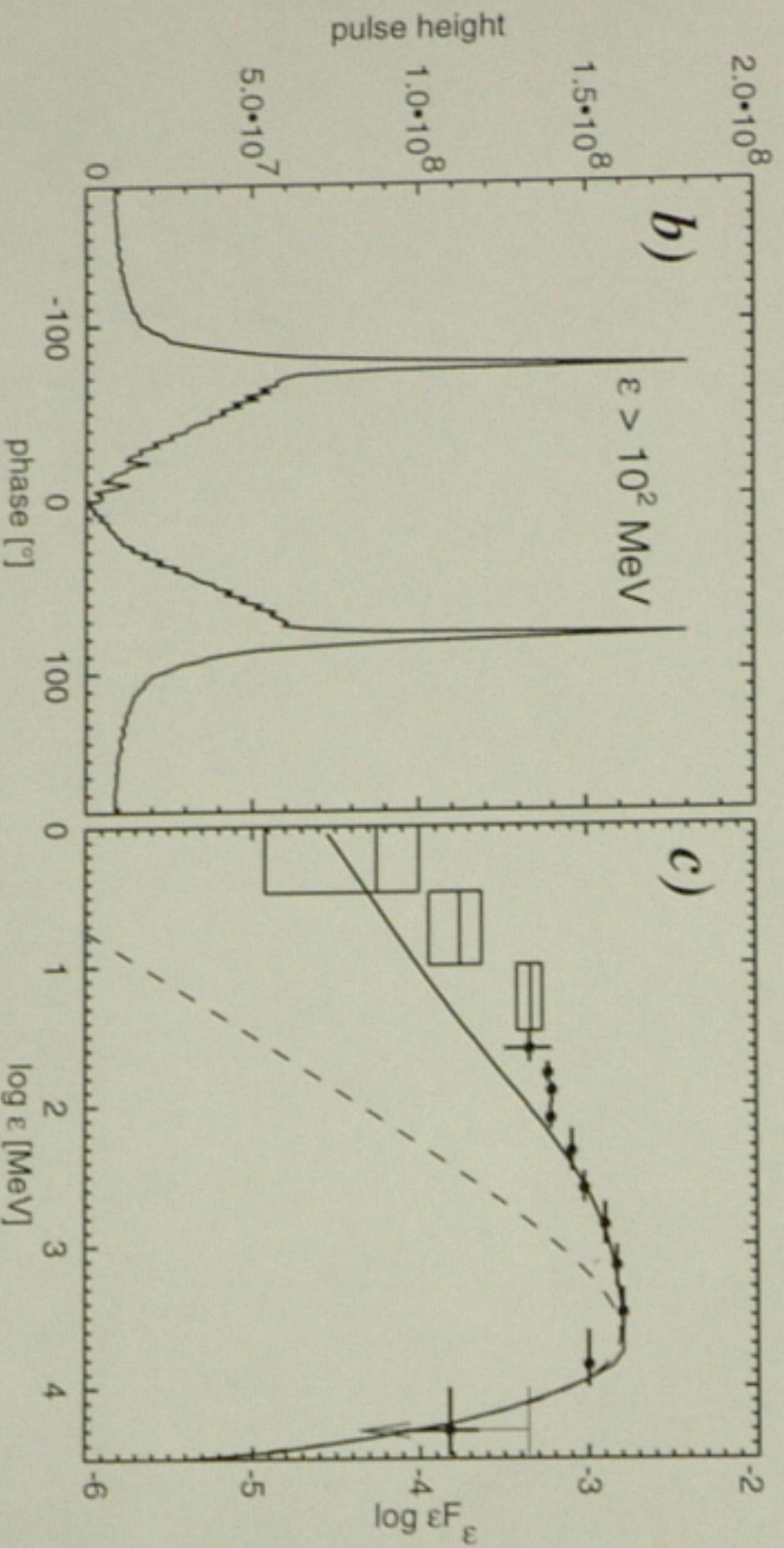
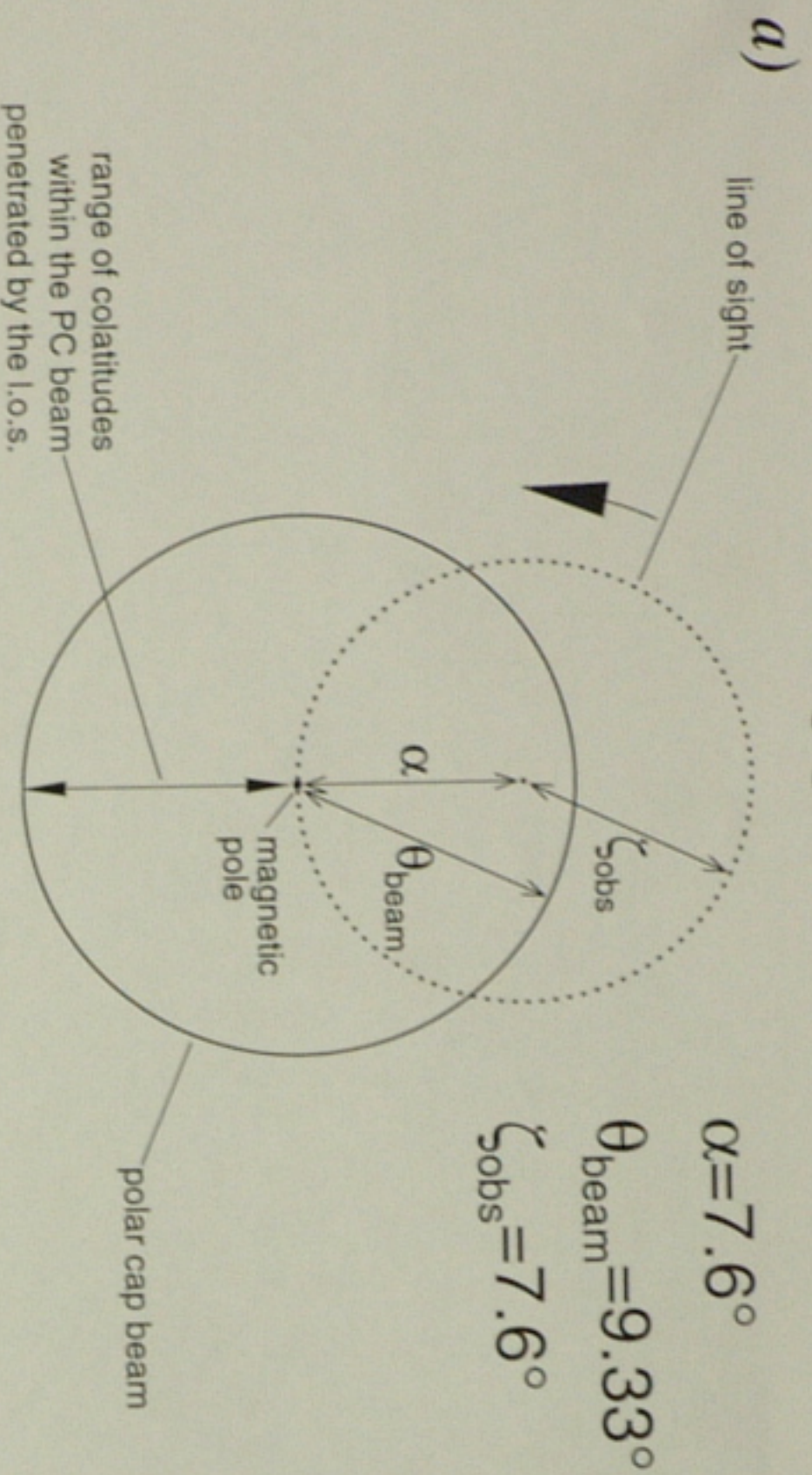


Figure 3: **a)** Viewing geometry assumed to calculate the profile and the spectrum shown in panels b and c. The line of sight crosses the polar cap beam (solid circle) along the dotted trajectory. **b)** Pulse profile calculated for $\epsilon > 10^2 \text{ MeV}$. **c)** Phase-averaged spectrum (solid line) overlotted on COMPTEL and EGRET data for the Vela pulsar. An instantaneous spectrum of CR with exponential cutoff due to monoenergetic particles is shown for reference (dashed line). **The modelled spectrum (solid line) assumes now a simple exponential shape instead of the super-exponential one. (Cf. the spectrum in Fig. 2.)**

2 Weakening of the leading peak

According to the polar cap model, the characteristic double-peak gamma-ray pulse profiles of pulsars arise as follows: when the line of sight enters the polar cap beam the leading peak is produced (LP); crossing inner parts of the hollow beam gives the bridge emission between the two peaks, and leaving the beam gives the trailing peak (TP) (see Fig. 2a and 3a).

Rotation of magnetosphere enhances the magnetic absorption of photons in the leading peak and weakens the absorption of the trailing peak (Dyks, Rudak 2002). This may be easily understood by inspection of Fig. 4, which shows the trajectory of leading peak photons (dashed curve on the left) and trailing peak photons (dashed curve on the right) in the frame rigidly corotating with the star.

Therefore, the leading peak in a pulse profile disappears at a lower photon energy than the trailing peak, an effect noticed among the brightest EGRET pulsars (Thompson 2001). Fig. 5 shows this effect for the nearly aligned model of the Vela pulsar (see two lowermost panels in the middle column).

Due to the stronger absorption at the leading peak, a higher number of low-energy synchrotron photons emerges at the LP than at the TP. This is the reason for a dominance of the LP over the TP below ~ 100 MeV, noticeable in Fig. 5. A qualitatively similar inversion of peak intensities takes place in the gamma-ray profile of the Vela pulsar (Kanbach 1999; Thompson 2001).

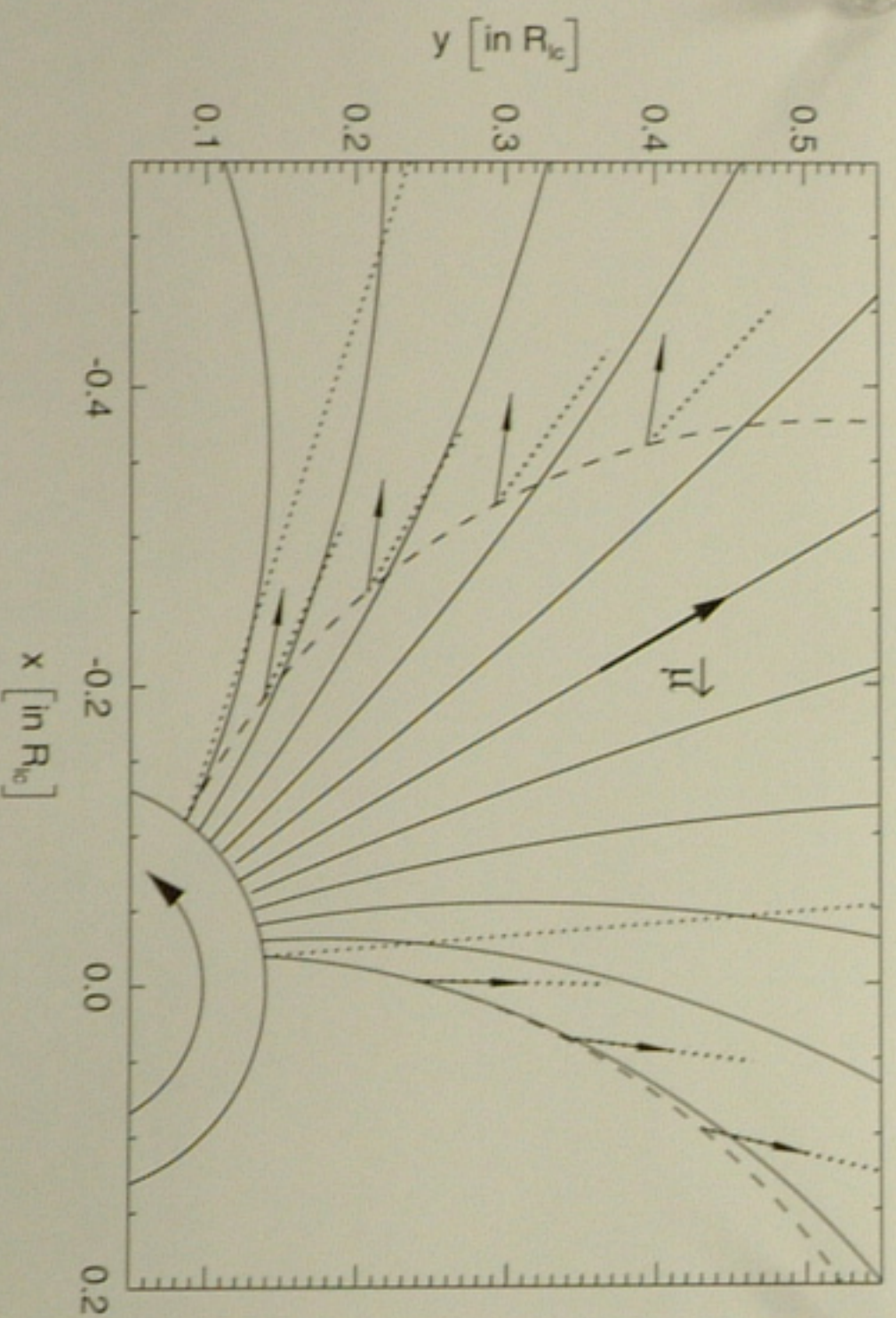


Figure 4: Top view of orthogonally rotating pulsar with the spin period $P = 1.5$ ms. The magnetic field lines are approximated with the static-like dipole of the magnetic moment $\vec{\mu}$. Two photon trajectories (starting from two opposite points on the polar cap) in the corotating frame (CF) are marked with two long dashed lines. These are the prototypes of the leading peak (on the left) and the trailing peak (on the right). Note that photons of the leading peak cross the magnetic field at much larger angles than photons of the trailing peak.

3 Step-

For the near leading peak place at high assumed h high inclination cutoff's energy pronounced, as a step in step occurs meV. Below leading and the trailing by a factor

4 Cham

Figure 6: The second pulse distribution the step-like

Another o tons is a peaks in t the case o models wi beam" mo higher em aligned ge beam tra If the e opposite spectrum beam", th

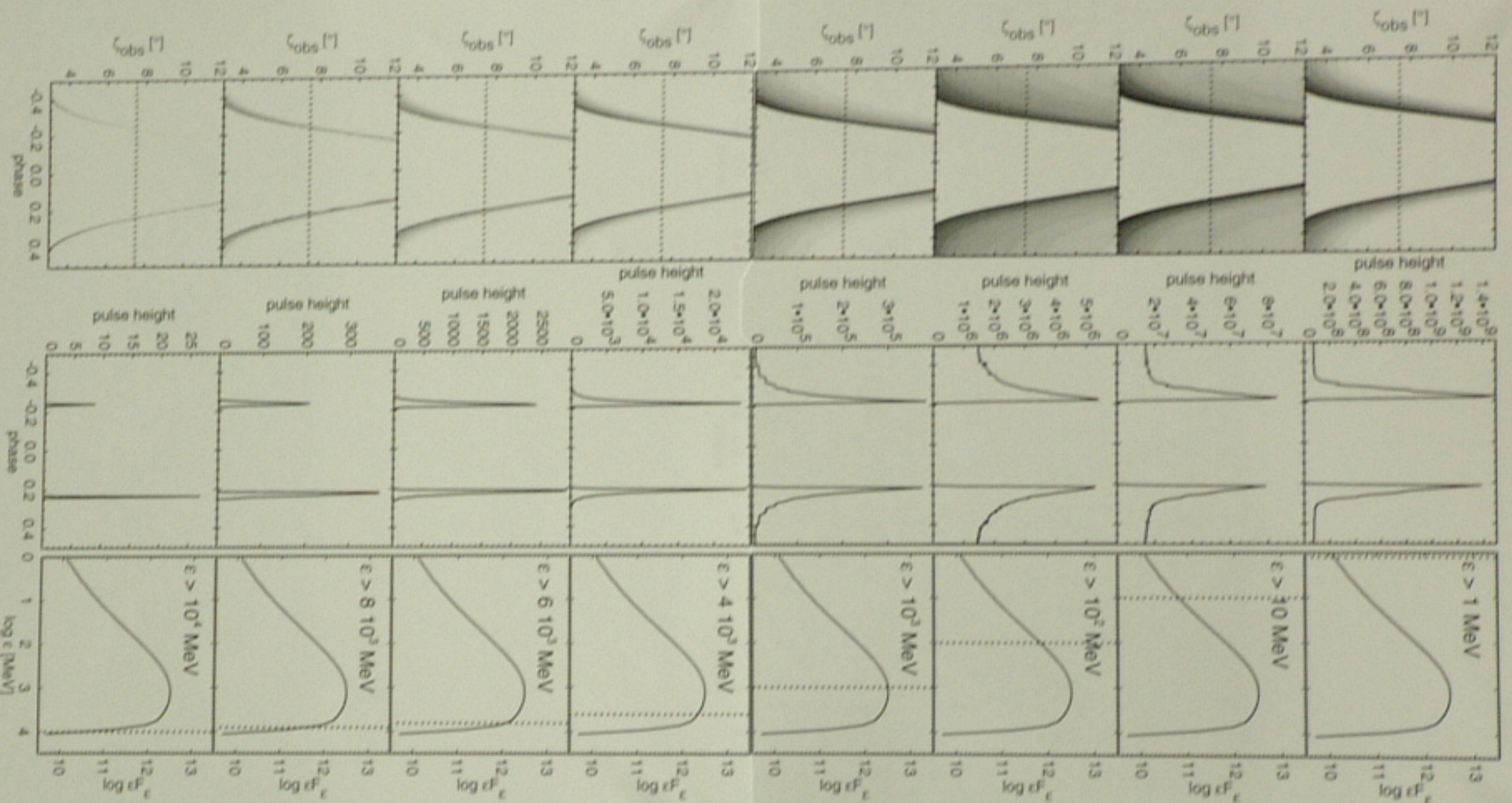


Figure 5: Directional and spectral gamma-ray characteristics calculated for the Vela pulsar with the angle α between the spin axis and the magnetic axis set $\alpha = 7.6^\circ$ (nearly aligned rotator). Eight rows are shown (the continuation in Fig. 5b), with three panels each. **Left column** shows the outgoing photons of energy $\epsilon > \epsilon_{\text{limit}}$ which are mapped onto the parameter space C_{obs} vs. ϕ , where C_{obs} is the viewing angle (between the spin axis and the l.o.s) and ϕ denotes the phase of rotation. **Middle column** shows the double-peak pulse profile formed with these photons when $C_{\text{obs}} = 7.6^\circ$ is chosen (yielding the peak-to-peak separation equal 0.42). **Right column** shows the phase-averaged energy spectrum (the flux level ϵF_ϵ in arbitrary units) for $C_{\text{obs}} = 7.6^\circ$ i.e. the same for all rows. Dotted vertical line indicates the part of the spectrum ($\epsilon > \epsilon_{\text{limit}}$) which contributes to the corresponding pulse profile on the left. The value of ϵ_{limit} increases from top to bottom.

profile and the spectrum
 ar cap beam (solid cir-
 ted for $\epsilon > 10^2$ MeV. c)
 OMPTEL and EGRET
 with exponential cutoff
 (dashed line). The mod-
 e exponential shape
 spectrum in Fig. 2.)

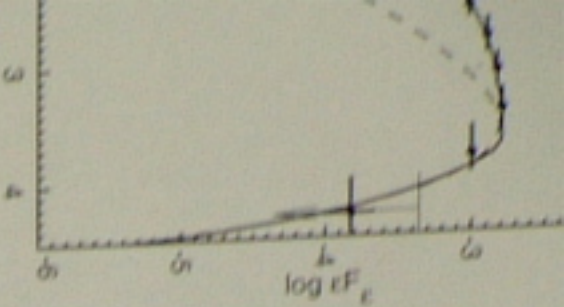
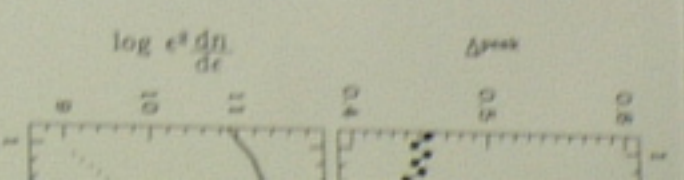


Figure 7: U
 emission p
 B, C and f
 few GeV is
 Lower pa
 peak as a
 dashed) an
 A, B, and



5 GEN

The high-e
 ing energy
 least four,
 their magn
 factors whi
 electrons a

Referenc

de Jager, C
 Dyks, J., R
 Dyks, J., R
 Harding, A
 Kanbach, C
 Thompson.

3 Step-like spectrum

For the nearly-aligned model of Vela, shown in Fig. 5, the fading of the leading peak can be discerned only when acceleration of electrons takes place at high altitudes, where the local corotation velocity is large (we assumed $h = 4R_{NS}$ in Fig. 5). However, for millisecond pulsars with high inclination angles α of magnetic dipole, the difference between cutoff's energy for the leading and for the trailing peak becomes pronounced, and may be noticeable even in the phase-averaged spectrum as a step nearby the HE cutoff. In the spectrum shown in Fig. 6 the step occurs at around 10^5 MeV, and the "ultimate" cutoff at $5 \cdot 10^5$ MeV. Below the step the spectrum consists of photons from both the leading and the trailing peak, whereas above the step only photons of the trailing peak contribute. At the step the level of spectrum drops by a factor of ~ 2 .

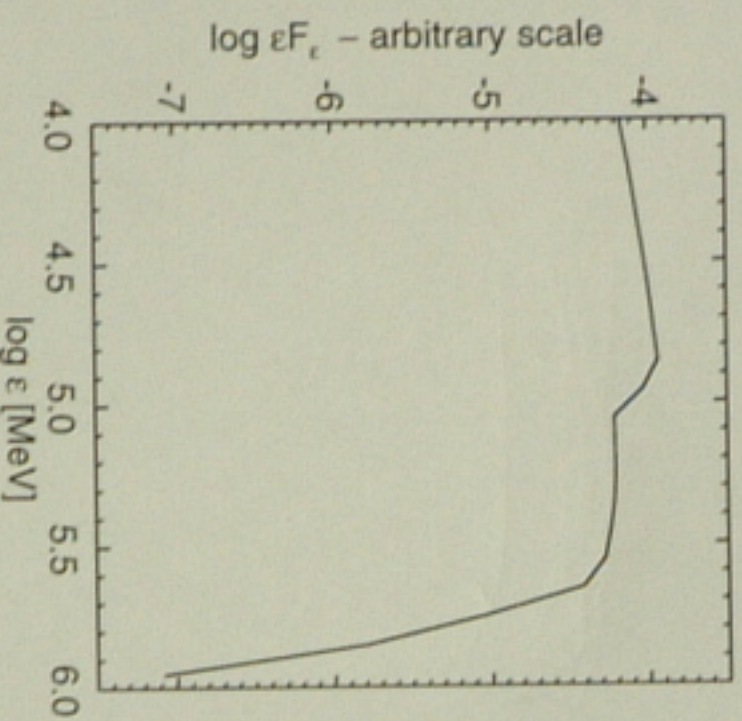


Figure 6: Theoretical "on-beam" spectrum of high-energy emission from a millisecond pulsar with $P = 2.3$ ms, $B_{pc} = 10^9$ G, and $\zeta_{obs} = \alpha = 60^\circ$. The density distribution of primary electrons was uniform along the polar cap rim. Note the step-like decline around ~ 100 GeV.

4 Change of peak separation

Another consequence of the magnetic absorption of high energy photons is a noticeable change in the separation Δ_{Peak} between the two peaks in the pulse profile, taking place near the HE spectral cutoff in the case of nearly aligned rotators (Fig. 7; Dyks & Rudak 2000). In models with electrons ejected only from a rim of the polar cap, ("hollow beam" models A, B, C in Fig. 7), the higher energy of photons requires

4 Change of peak separation

Another consequence of the magnetic absorption of high energy photons is a noticeable change in the separation Δ^{peak} between the two peaks in the pulse profile, taking place near the HE spectral cutoff in the case of nearly aligned rotators (Fig. 7; Dyks & Rudak 2000). In models with electrons ejected only from a rim of the polar cap, ("hollow beam" models A, B, C in Fig. 7), the higher energy of photons requires higher emission altitudes to avoid absorption. Because of the nearly aligned geometry, the slightly larger opening angle of the gamma-ray beam translates into a very clear increase in Δ^{peak} .

If the emission from the interior of the polar cap is included, just the opposite behaviour occurs: Δ^{peak} decreases near the HE cutoff in the spectrum (Model D in Fig. 7). This is because in this case of a "filled beam", the highest energy non-absorbed photons are emitted closer to the magnetic dipole axis.

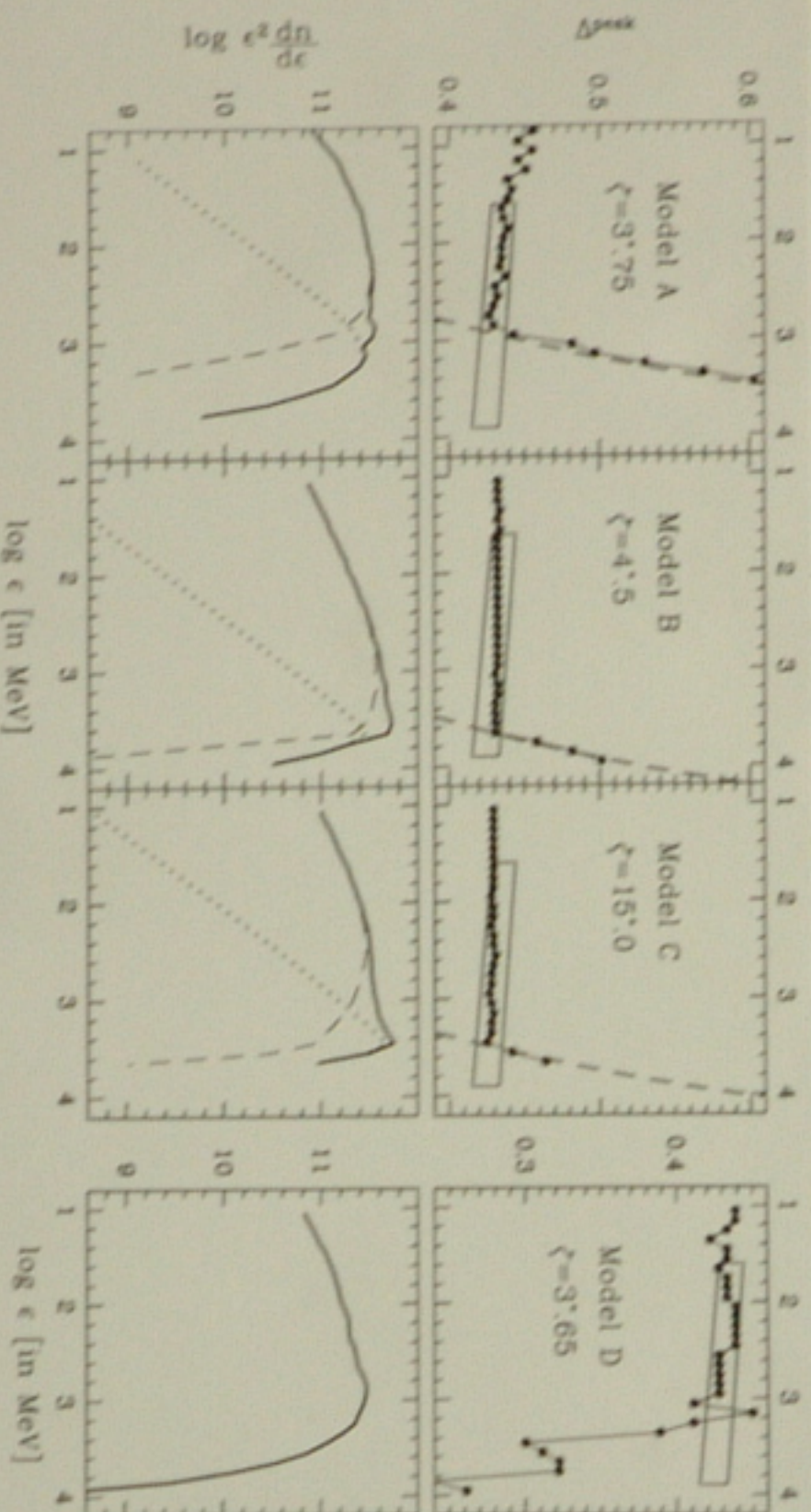


Figure 7: **Upper panels:** Phase separation Δ^{peak} versus photon energy ε of the emission peaks found with Monte Carlo calculations for hollow beam models A, B, C and for a filled beam model D (dots). The sharp change of Δ^{peak} above a few GeV is caused by magnetic absorption effects ($\gamma B \rightarrow e^\pm$).

Lower panels: Energy output per logarithmic energy bandwidth at the first peak as a function of photon energy ε (solid line). The synchrotron (long dashed) and the curvature (short dashed) components are marked for models A, B, and C. Figure from Dyks & Rudak (2000).